Cancer Science

WILEY

Cancer Science

ORIGINAL ARTICLE OPEN ACCESS

APE1 Attenuates ALK Tyrosine Kinase Inhibitors Sensitivity in NPM1-ALK Positive Anaplastic Large Cell Lymphoma

Zheng Liu[1,2] | Xinming Jing[1] | Dong Li[2] | Lingbo Bao[2] | Yi Liu[3] | Ruyi Hang[1] | Xunjie Kuang[1] | Ziqi Jiang[1] | Xiaoyan Dai[1] | Xueling Tong[1] | Gianluca Tell[4] | Mengxia Li[1]

[1]Cancer Center, Daping Hospital & Army Medical Center of PLA, Army Medical University (Third Military Medical University), Chongqing, China | [2]Department of Oncology, The General Hospital of Western Theater Command, Chengdu, China | [3]Department of Hypertension and Endocrinology, Center for Hypertension and Metabolic Diseases, Daping Hospital, Army Medical University (Third Military Medical University), Chongqing, China | [4]Laboratory of Molecular Biology and DNA Repair, Department of Medicine, University of Udine, Udine, Italy

Correspondence: Mengxia Li (limengxia@tmmu.edu.cn)

Received: 31 January 2025 | **Revised:** 18 April 2025 | **Accepted:** 9 July 2025

Funding: This work was supported by Postgraduate Research & Practice Innovation Program of Chongqing Province, CYB240289; National Natural Science Foundation of China; the Talent Innovation and Capacity Building Program (Organized Research) of Army Medical Center of PLA, ZXYZZKY07.

Keywords: ALCL | ALK-TKI | APE1 | NPM1-ALK | TKI sensitivity

ABSTRACT

Anaplastic lymphoma kinase (ALK), a tyrosine kinase receptor of the RTK insulin superfamily, was named after its initial identification in anaplastic large cell lymphoma (ALCL). Following a reciprocal chromosomal translocation with nucleophosmin 1 (NPM1), ALK protein is abnormally expressed, promoting the malignant transformation of T cells into a more aggressive lymphoma. The inhibition of ALK activity could therefore benefit ALK+ ALCL patients. Despite the market availability and success of ALK tyrosine kinase inhibitors (TKIs), real-world ALK+ ALCL patients exhibit significant heterogeneity in terms of disease stage at first diagnosis, tumor progression, and responses to medication. This indicates a need for more detailed differentiation of ALK+ ALCL patients in clinical practice. Here, we discovered that apurinic/apyrimidinic endonuclease-reduction/oxidation factor 1 (APE1/REF1), an interacting partner of NPM1, could stabilize NPM1-ALK fusion protein oligomers and enhance ALK tumor-promoting activity and growth, decreasing cell sensitivity to ALK-TKIs. Our results also reveal that disruption of the interaction weakens cell growth and augments the therapeutic efficacy of crizotinib and alectinib, ALK-TKIs, against ALK+ ALCL. Thus, high expression of APE1 indicates a faster growth of ALK+ ALCL; targeting this interaction may potentially achieve improved therapeutic outcomes, providing a reference for more precise treatment of ALK+ ALCL patients in clinical practice.

Abbreviations: ALCL, anaplastic large cell lymphoma; ALK, anaplastic lymphoma kinase; APE1, apurinic/apyrimidinic endonuclease 1; BER, base excision repair; NPM1, Nucleophosmin 1; TKI, tyrosine kinase inhibitor.

Zheng Liu, Xinming Jing, and Dong Li are contributed equally to this work.

1 | Introduction

Anaplastic large cell lymphoma (ALCL) is an aggressive mature T-cell tumor frequently found in children and young adults, with about 50%–80% of cases expressing anaplastic lymphoma kinase (ALK) [1]. ALK is, in fact, named for its initial identification in ALCL [2]. Wild-type ALK is normally expressed at a low level in neural cells of the cerebral cortex, hypothalamus, and cerebellum, etc. [3] Chromosomal abnormalities, namely translocations and inversions, can result in the expression of ALK protein fused with additional factors, such as nucleophosmin-1 (NPM1), echinoderm microtubule-associated protein-like-4 (EML4), and tropomyosin-3 (TPM3) across different tumor types [4–6]. In ALCL, the most frequently observed event is fusion of *Alk* on chromosome 2 with *Npm1* on chromosome 5, genetically defined as t(2;5) (p23;q35), creating a fusion gene, *Npm1-alk*. Oligomerization molecular chaperone (amino acids 1–116) of the NPM1 segment mediates dimerization of the NPM1-ALK fusion protein [7, 8]. As a general cancer-driving protein, ALK activates downstream growth pathways, such as the PI3K/Akt, ERK1/2, and JAK/STAT, promoting tumor occurrence and development [9–12]. Inhibition of ALK benefits ALCL patients, with some clinical trials finished [13–15] and several clinical studies ongoing (ChiCTR2000029373, NCT03505554, etc.). ALK+ ALCL is categorized as a distinct disease in the 2008 WHO classification system, with a higher survival rate than ALK− ALCL patients [16]. Despite being classified separately, ALK+ ALCL patients show significant heterogeneity in disease stages at initial diagnosis, progression, and responses to medication, underscoring the need for the identification of novel patient-specific factors that inform target classification and therapeutic strategies [17, 18].

Apurinic/apyrimidinic endonuclease-1 (APE1), a crucial enzyme in DNA damage repair pathways and cellular responses, participates in base excision repair (BER), transcriptional regulation, redox reactions, RNA metabolism, and various other cellular processes [19, 20]. Recently, the role of APE1 in tumors has gained attention [21], with some studies finding that APE1 plays a significant role in tumor development and sensitivity to radiotherapy and chemotherapy in many cancers [22–25]. The N-terminal region of APE1 mediates many of its protein–protein interactions, as well as its subcellular localization and post-translational modifications [26–29]. Moreover, prior studies have indicated an interaction of APE1 and NPM1 in the rRNA quality control process, suggesting a possible link between the repair protein and the NPM1-ALK fusion protein [20]. In light of the importance of APE1 in cancer biology, as well as its association with NPM1, we were wondering what role this multifunctional protein plays in ALK+ ALCL.

2 | Material and Methods

2.1 | Reagents

Antibodies against APE1 were purchased from Abcam (MA, USA); NPM1, NPM-C were purchased from Santa Cruz (Shanghai, China); ALK, phospho-ALK, Stat3, ERK1/2, Akt, phospho-p44/42 (Thr202/Tyr204), phospho-Akt, phospho-Stat3 (Tyr705), and normal rabbit IgG were purchased from Cell Signaling Technology (Danvers, MA, USA). Crizotinib and alectinib were obtained from MedChemExpress (Shanghai, China).

2.2 | Cell Culture and Treatments

All cells were purchased from Biospes (Chongqing, China) in September 2020 and were authenticated by STR in November 2020. SU-DHL-1 and Karpas-299 cells were maintained in RPMI 1640 medium (Procell, China), supplemented with 10% fetal bovine serum and 1% penicillin–streptomycin; 293T cells were maintained in DMEM. Passaging of the cells was performed with 0.25% trypsin–EDTA (Procell). All cell lines were tested for mycoplasma contamination at regular intervals and results always showed negative. Protein knockdown (KD) or overexpression (OE) experiments were conducted using lentivirus or plasmid. The methods that lentivirus was packaged, transfection, and verification were stated before [30].

2.3 | IHC

Acquisition of all samples in this research was approved by the Ethics Committee of Daping Hospital. Briefly, the formalin-fixed and paraffin-embedded (FFPE) ALCL clinical specimen sections were obtained from the Department of Pathology, Daping Hospital. Xenograft sections were prepared with an intelligent program-controlled automatic hydroextractor (Taiva Technology, Hubei, China). After dewaxing, heat-induced epitope retrieval (HIER) was conducted with EDTA (pH 8.0) or slightly acidic buffer citrate (pH 6.0). After 10 min of incubation at room temperature with endogenous peroxidase blocker (MXB, China), sections were incubated with specific antibodies at 4°C overnight. The next day, sections were incubated with HRP-coupling second antibody at 37°C for 30 min and stained with DAB. Nuclear was stained with hematoxylin. The expression of in the dicated protein was evaluated with ImageJ based on the *H* Score criteria (*H* Score = 1 × percentage contribution of Low Positive +2 × percentage contribution of Positive +3× percentage contribution of High Positive).

2.4 | Westernblot

Cells and xenograft tissue were homogenized in T-PER Tissue Protein Extraction Reagent (Thermo Fisher, USA), supplemented with a proteinase and phosphatase inhibitor mixture (Thermo), then mixture was incubated at 4°C for 20 min and centrifuged for 15 min at 18000 g after ultrasonication to get whole-cell extraction. The protein levels in the extracts were quantified using NanoDrop One Microvolume UV–Vis Spectrophotometer (Thermo). For the preparation of a 10% separating gel (15 mL total volume), combine 6 mL of ddH_2O, 4.95 mL of acrylamide mix (30% acrylamide solution and 2% bis-acrylamide solution at 29:1 ratio), 3.75 mL of 1.5 M Tris–HCl (pH 8.8), 0.15 mL of 10% SDS, 0.18 mL of 10% APS, and 12 μL TEMED. Mix thoroughly and pour into the gel-casting apparatus to polymerize. For the 4% stacking gel (3 mL total volume), combine 2.1 mL of ddH_2O, 0.5 mL of the same acrylamide mix, 0.38 mL of 0.5 M Tris–HCl (pH 6.8), 0.03 mL of 10% SDS, 50 μL of 10% APS, and 5 μL TEMED. For western blotting, whole-cell extracts (25–30 μg/

lane) were resolved on wells and run it by electrophoresis at 110 V until the dye front reaches the bottom of the gel. For membrane transfer: 100 V for 90–120 min, proteins were transferred to a nitrocellulose membrane (0.2 μm; Bio-Rad, CA, USA) in 25 mM Tris-base, 190 mM glycine and 20% methanol with a semidry blotter. 4%–20% gradient gels were purchased from ACE (ACE Biotechnology, China). Membranes were blocked with 5% bovine serum albumin (BSA) or defatted milk for l.5 h, then incubated with a primary antibody (suggested dilution rate) and secondary antibody sequentially. Protein bands were detected using a clarity max western ECL substrate (Bio-Rad), and light emission was captured on a chemidoc touch imaging system (Bio-Rad).

2.5 | CO-Immunoprecipitation

Whole-cell extracts were prepared with Cell lysis buffer for IP (Beyotime, China) without ultrasonication and incubated with a particular antibody or normal rabbit IgG and A/G magnetic beads at 4°C temperature for 12–16 h. Magnetic beads were collected with a magnetic rack. After washing with PBST for five times, beads were homogenized with SDS-PAGE sample loading buffer and boiled for 5 min in a metal bath at 95°C. Next steps were conducted as WB.

2.6 | Immunofluorescence

Before the experiment, ALCL cells were washed 3 times with PBS and maintained on glass bottom cell culture dishes (NEST, China), then centrifuged the dishes for 5 min at 750***g*** in a refrigerated centrifuge (Shuke, Sichuan, China). After fixation in methanol at room temperature for 2 h, cells were permeabilized with 0.02% Triton X-100 for 15 min, and then blocked with goat serum for 1 h. Then cells were incubated with the corresponding primary antibody overnight at 4°C in a humidity chamber. The next day, cells were incubated with the secondary antibodies (1:1000), which were conjugated to relevant Alexa Fluor fluorescent dye for 1 h at room temperature. Nuclear was counterstained with 4′,6-diamidino-2-phenylindole (DAPI) (Roche, Switzerland) for 5 min. Dishes were visualized for immunofluorescence with a laser scanning confocal microscope (Zeiss, Germany).

2.7 | FLOW Cytometry

Cell apoptosis was measured by an Annexin V-PE/7-AAD Apoptosis Detection Kit (Bestbio, China). Briefly, cells were plated in 6-well plates; after 72 h of treatment, cells were harvested and washed with PBS. All steps were conducted under the guidance of the kit. Apoptotic cells were determined by flow cytometry (Beckman Coulter, USA); 10,000 events were recorded for analysis with CytExpert 2.6 software.

2.8 | Multiplex Immunohistochemistry

MIHC staining was performed on 2 μm histologic tumor sections from FFPE tumor samples with the 7-Color mIHC Kit (Panovue, China). The IF markers were grouped into the panel consisting of ALK (1:500), APE1 (1:2000), pALK (1:200), pSTAT3 (1:200), and pERK (1:300). Briefly, all steps are conducted following the specifications of the 7-Color mIHC kit. The deparaffinized and epitope retrieval procedures were the same as IHC. Only one antigen was incubated each round, followed by epitope retrieval and protein blocking again. After nucleus staining, slides were visualized using the phenoimager Fusion (Akoya Biosciences).

2.9 | PLA

Proximity Ligation assay (PLA) was performed following Duolink PLA manufacturer's instructions (Sigma, USA). Cells were plated on glass bottom cell culture dishes 1 day before experiments. After fixation and permeabilization (the same as IF), cells were incubated with rabbit ALK antibody, mouse APE1 antibodies, or no antibody overnight at 4°C, followed by incubation with secondary antibodies conjugated with PLA probe at 37°C for 1 h. Then, ligation and amplification were performed following construction (Sigma, USA). 293T cells uninfected by NPM1-ALK lentivirus were used as a biological negative control to detect the specificity of primary antibodies; technical negative control (NC) was set with no primary antibody used during the experiment to exclude background signals. Lastly, imaging was conducted with a confocal microscopy (TCS SP5, Leica, Germany).

2.10 | Xenograft Studies

Three-to-four-week-old male NCG mice (T001475) were purchased from GemPharmatech (Jiangsu, China). All mice were maintained in a temperature-controlled (22°C–25°C), pathogen-free environment and had free access to food and water in Animal Centre of Daping Hospital. Mice were randomly divided into four groups when they reached the age of 4 weeks and an average body weight of 25 g. For subcutaneous xenografts, 5×10^6 SU-DHL-1 APE1 wt or $APE1^{K4pleA}$ (the Lys27/31/32/35 of APE1 were replaced by Ala) cells in 100 μL of PBS were injected subcutaneously into mice respectively after grouping. From the 7th day post-injection, mice body weight and tumor dimensions were assessed and documented every other day. When tumor volume reached 200 mm^3, mice were treated with crizotinib (50 mg/kg) or a placebo; crizotinib was administrated by intragastric administration every day. Placebo consisted of saline and PEG300 in a 1:1 configuration. Maximum and minimum values within the group were excluded. All mice were euthanized, and tumors were surgically dissected at a humane endpoint.

2.11 | Statistical Analysis

Statistical data were expressed as mean ± SD. All of the statistical analyses were assessed by GraphPad Prism 9.5.1 software and ggpubr package with R 4.3.2; comparisons among groups were done by chi-square test, the independent sample two-sided Student *t* test, and one-way ANOVA test. $*p < 0.05$, $**p < 0.01$, $***p < 0.001$, $****p < 0.0001$, ns represents no statistical differences. According to previous experience in the laboratory, we chose pre-specified effect sizes considered to be biologically significant. No blind analysis was performed in this study.

3 | Results

3.1 | APE1 Is Highly Correlated With Later Lugano Stage and NPM1-ALK Activation in ALK+ALCL Patients

To identify candidate novel determinants, we first employed immunoprecipitation (IP) with ALK antibodies and used proteomic studies to determine proteins bound to the NPM1-ALK fusion protein from SU-DHL-1 cell extracts. We found that NPM1-ALK captured the multifunctional protein APE1 (Figure 1A). We next collected pathological sections of ALCL patients from our center between 2012.07 and 2023.08, of which 35 of 44 had available pathological specimens (Table 1). Then IHC staining was performed for APE1 and NPM1-ALK; representative pictures were shown (Figure 1B), and NPM1-ALK expression was validated by a specified antibody (Figure S1A). Combined with the patients' clinical characteristics, we found that in patients with high expression of APE1, there was a significant association with a later clinical stage at initial diagnosis, while there was no such trend observed in ALK- ALCL (Figure 1C). Furthermore, we observed that tumors with high APE1 expression exhibited correspondingly elevated Ki-67 expression, and serum LDH levels in these patients also trended higher (Figure 1C). Interestingly, NPM1-ALK appears to reside more in the nucleus in APE1-high expressing patient samples compared to APE1-low expressing material, which may be helpful to its better performance of function (Figure S1B). Details of the APE1 IHC *H* Score are listed in Table S1. Meanwhile, mIHC was introduced on ALK+ ALCL paraffin sections from patients; APE1, NPM1-ALK, and its downstream proteins were stained, and NPM1-ALK was used to distinguish tumor tissue. Results showed that patients with high APE1 expression also have higher expression of pALK as well as its downstream signaling proteins pSTAT3 and pERK. Focusing on a single sample, we differentiated ALK+ ALCL cells by APE1 staining intensity index; results showed the same trend in intratumor heterogeneity (Figure 1D–F). These strongly suggest that APE1 plays a crucial role in NPM1-ALK+ ALCL.

3.2 | APE1 OE Activates NPM1-ALK and Reduces ALK-TKI Sensitivity

To figure out what happens in ALK+ ALCL, we overexpressed (OE) APE1 in ALK+ ALCL cell lines (SU-DHL-1 and Karpas-299) using a lentivirus system. Specifically, we found that infection of the APE1-FLAG OE lentiviral particle, but not the negative control virus (NC), resulted in an increased cell growth velocity (Figure 2A). Then a series of biological endpoints were assessed by WB, and it showed an overactivation trend (Figure 2B).

Since APE1 activates NPM1-ALK, we determined the effect of APE1 OE on ALK activation in the presence of an ALK-TKI, that is, crizotinib, alectinib, which were used to control ALK activity for ALK+ ALCL patients clinically in China, Japan, and the USA. Increasing concentrations of each inhibitor were added, and cell viability was assessed by a cell counting kit. Results showed that the IC50 of APE1 OE cells was significantly higher than NC in two cell lines, especially crizotinib (Figure 2C). NPM1-ALK positive ALCL cells were treated with 300 nM crizotinib or 100 nM alectinib, and then cell viability was evaluated by CCK-8 Kit at different time points (0, 24, 48, and 72 h). Results showed that OE of APE1 significantly weakened the inhibitory effect of ALK-TKIs. ALK-related downstream cascades showed the same tendency (Figure 2E). After that, the ALK-TKI concentration gradient was set; although phosphorylation of ALK was inhibited by crizotinib, OE of APE1 resulted in a 30% dampened inhibitory effect at a concentration of 300 nM (Figure S2), indicating impaired efficacy of the therapeutic inhibitors in the presence of higher APE1.

Previous studies of ALK revealed that oligomerization of the ALK fusion protein is vital for its activation, such that monomerization of the ALK intracellular domain via an inducible system inhibited ALK phosphorylation [31]. Interestingly, we observed that, while APE1 OE associated with increased oligomerization of the ALK fusion protein, knockdown of APE1 had the opposite effect (Figure 2F). Notably, we found that the oligomer-monomer equilibrium of NPM1-ALK is dynamically regulated by APE1, which stabilizes its oligomeric conformation. Upon APE1 knockdown (KD), a marked decline in NPM1-ALK oligomers was accompanied by a proportional rise of NPM1-ALK monomers. Quantitative immunoblotting confirmed these reciprocal changes, with relative levels of both oligomeric and monomeric NPM1-ALK explicitly quantified (Figure 2F). These findings indicate that APE1 likely regulates NPM1-ALK activity via stabilization of the NPM1-ALK oligomer.

3.3 | APE1 Interacts With NPM1-ALK Fusion Protein in Nucleus

Given the previously described interaction between the ALK fusion partner NPM1 and APE1 [20], we therefore examined whether APE1 was consistently observed in a NPM1-ALK fusion protein complex in ALCL. Specifically, we performed CO-IP experiments using SU-DHL-1 and Karpas-299 cell extracts with anti-APE1 or anti-ALK antibody, followed by immunoblotting (IB). Both cell lines were found to possess a robust complex connection between the two proteins (Figure 3A,B). To further confirm the interaction, we repeated the experiment in 293 T cells using APE1 and NPM1-ALK protein–expressing lentivirus systems, obtaining the same results (Figure 3C and Figure S3A). After knocking down APE1 (Figure S3B), we re-expressed an APE1 variant lacking the 33 N-terminal residues (N△33APE1) and mutants APE1^{K4pleA}, where the replacement of the Lys27/31/32/35 by Ala residues was believed to disrupt the interaction sites while neutralizing the positive charges of the side chains [32]. After that, we no longer observed the robust interaction between APE1 and NPM1-ALK (Figure 3A–C), in accord with mapping studies of the APE1 and NPM1 binding requirements [20]. Meanwhile, we also used inhibitors targeting the APE1 redox region (E3330) and endonuclease region (CRT0044876 and inhibitor III), which were located after the N-terminal; results showed no influence on ALK-related downstream pathways (Figure S4).

Double immunofluorescent detections revealed co-localization of APE1 and NPM1-ALK proteins in SU-DHL-1 and Karpas-299 cells in both the cytoplasm and nucleus, whereas antibodies

A

Mass spectral peptide count

Protein name	Unique peptides
IGF2BP1	18
APEX1	15
HNRNPC	15
NPM1	12
ALK	11
ARG1	5
RPLP2	5
ZCCHC3	4
HBS1L	3
GTF3C2	3
HIRIP3	3

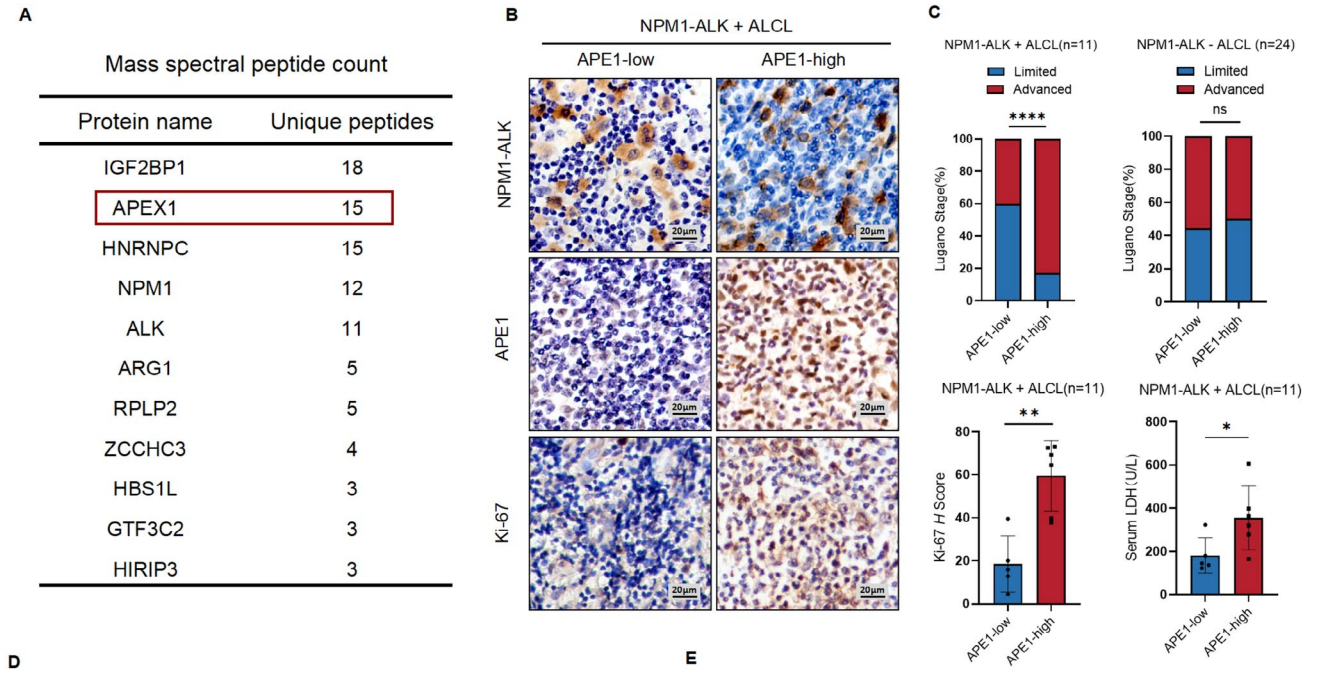

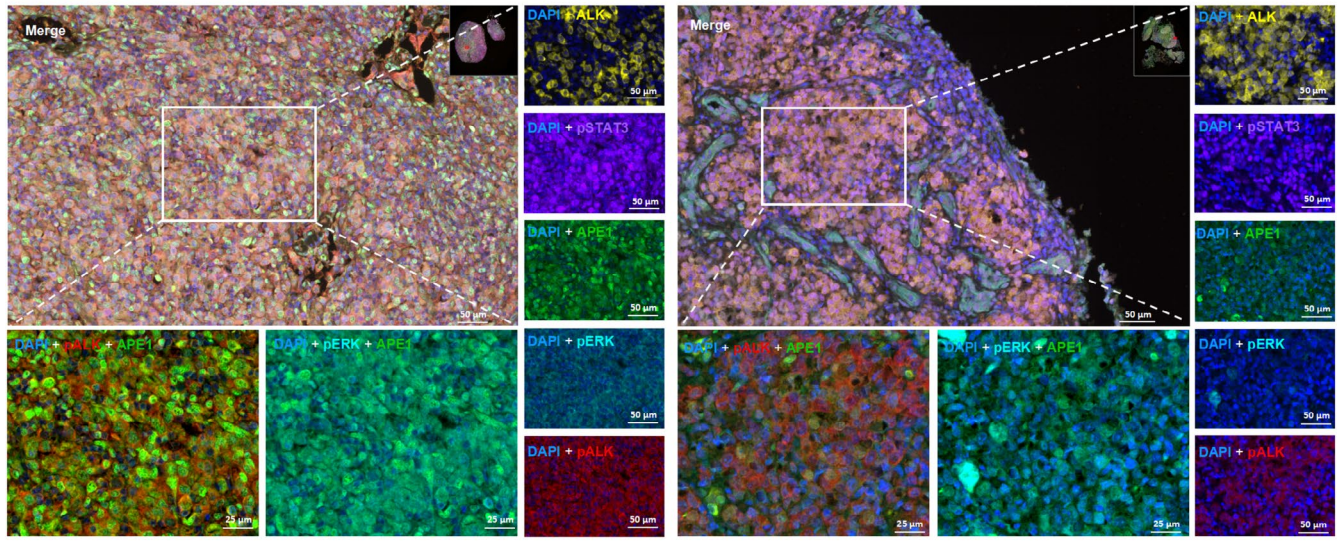

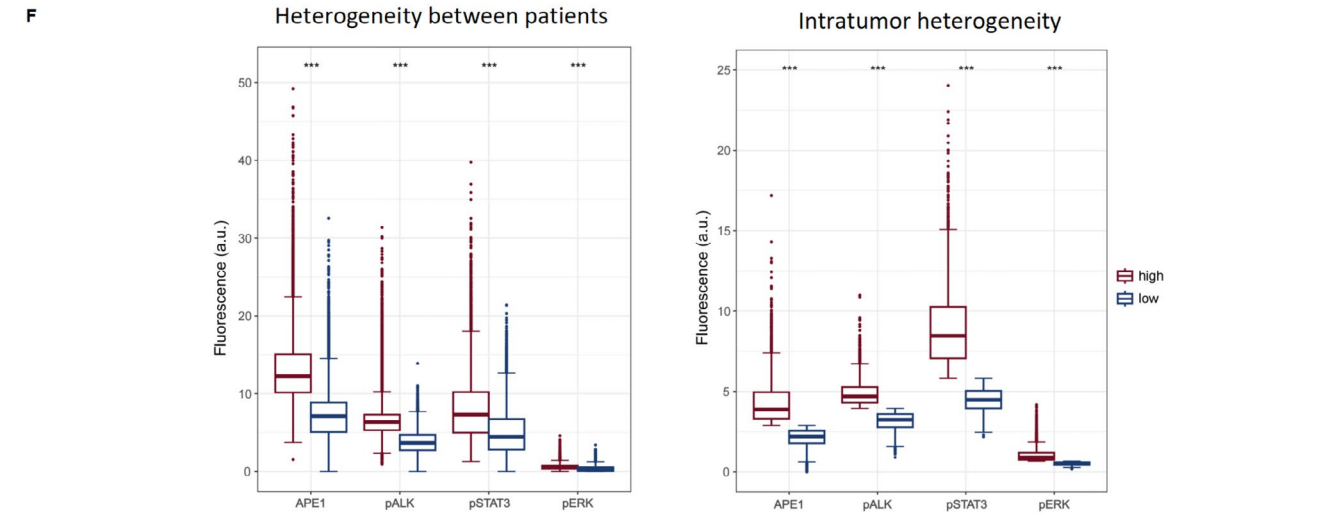

FIGURE 1 | Legend on next page.

FIGURE 1 | APE1 is highly correlated with later Lugano stage and NPM1-ALK activation in ALK+ALCL patients. (A) LC–MS/MS results of protein outcomes after immunoprecipitation with ALK antibody in SU-DHL-1 cells showing APE1 and NPM1. (B) Representative immunohistochemical staining with APE1, NPM1-ALK, or Ki-67 antibody in ALK+ALCL samples. Scale bars, 20 μm. (C) APE1 and Ki-67 expression were quantified by immunostaining, and their *H* score was assigned. Samples above average APE1 *H* score were defined as APE1-high, and vice versa. The clinical characteristics of the patients were based on the Lugano Revised Staging System (2014). Ki-67 H scores and serum LDH of patients were counted between APE1-low and APE1-high groups. ALK+ ALCL, $n = 11$; ALK- ALCL, $n = 24$. (D, E) APE1, NPM1-ALK, pALK, and pSTAT3 expression levels were visualized by multiplex immunofluorescence (mIHC). APE1 is highly expressed in (E), lower expressed in (F). Scale bars, 20 μm. (F) Phenochart and QPATH software were introduced to evaluate the intensity of fluorescence in each channel based on single cells. Statistical analysis and visualization were conducted by the ggpubr package with R 4.3.2. *$p < 0.05$, **$p < 0.01$, ***$p < 0.001$, ****$p < 0.0001$.

TABLE 1 | Clinical characteristics of ALCL patients.

		Patients	
	All, (No. %)	**ALK positive**	**ALK negative**
Characteristic	35	11	24
Patients			
Median age, years (range)	54 (23–70)	39 (23–68)	66 (31–70)
Sex			
Male	26 (74)	9 (82)	17 (71)
Female	9 (26)	2 (18)	7 (29)
Smoking history			
Never	20 (57)	6 (55)	14 (58)
Remote former smoker	3 (9)	1 (9)	2 (8)
Current smoker	12 (34)	4 (36)	8 (33)
Drink history			
Never	27 (77)	10 (91)	17 (71)
Light	4 (11)	0	4 (16)
Heavy	4 (11)	1 (9)	3 (13)
Stage at diagnosis (Lugano 2014)			
Limited (I and II)	15 (43)	4 (36)	11 (46)
Advanced (III and IV)	20 (57)	7 (64)	13 (54)
IPI score			
0	4 (11)	2 (18)	2 (8)
1	10 (29)	3 (27)	7 (29)
2	12 (34)	4 (36)	8 (33)
3	7 (20)	1 (9)	6 (25)
4	2 (6)	1 (9)	1 (4)

against the unique C-terminal region of NPM1 revealed only nucleolar localization of the endogenous (non-fusion) protein (Figure 3D). Lastly, APE1 wt and APE1^{K4pleA} were re-expressed in APE1 knocked-down HEK 293T cell lines using a lentivirus system; PLA studies confirmed that the interaction between NPM1-ALK and APE1 wt (wild-type) happens in the nucleus. APE1^{K4pleA} showed a significantly fewer and weakened Duolink complexes (Figure 3E); statistical analysis of PLA is shown.

3.4 | Interaction Site Mutation of APE1 Attenuated Phosphorylation of NPM1-ALK and Enhanced Tumor Inhibitory Effect of ALK-TKI

To figure out what happened when this interaction was weakened, we evaluated cell viability using a CCK-8 assay; results showed that in both ALK+ALCL cell lines, the APE1^{K4pleA} group grew clearly slower than the APE1 wt group (Figure 4A). Mutation of APE1 led to a reduction in NPM1—ALK oligomers

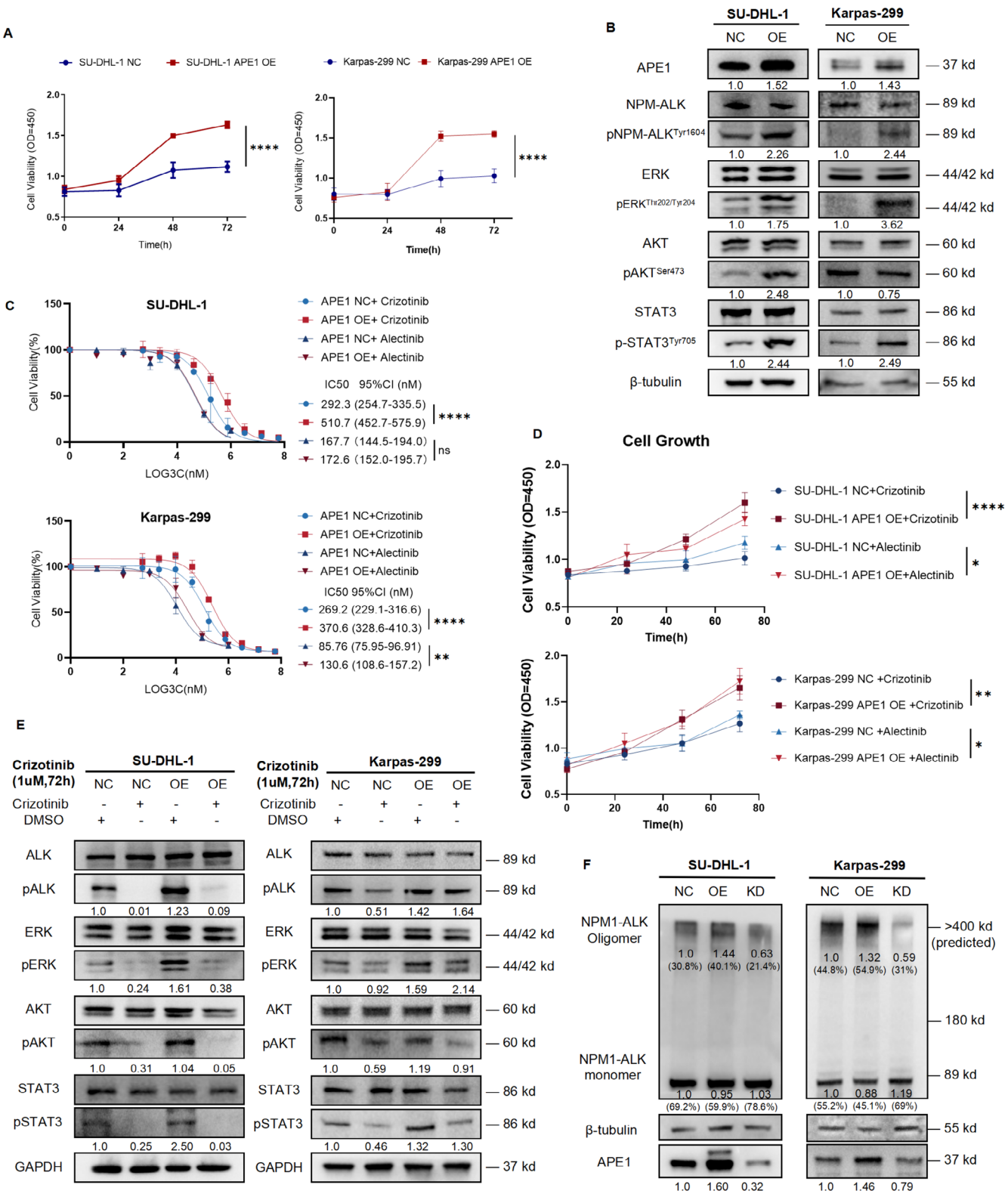

FIGURE 2 | APE1 OE activates NPM1-ALK and reduces ALK-TKI sensitivity in ALK+ ALCL. (A) APE1 was overexpressed in SU-DHL-1 and Karpas-299 cells with a lentivirus system. Cell viability was evaluated by a CCK-8 kit at the specified time points. (B) WB analysis performed on APE1 OE and NC ALK+ ALCL cell line; ALK and its downstream biological en-points were assessed. Bands were normalized on β-tubulin. (C) ALK-TKI IC50 of APE1 OE and NC ALK+ ALCL cells is evaluated by a CCK-8 kit. Cells were treated with crizotinib or alectinib for 72 h. (D) NPM1-ALK positive ALCL cells were treated with 300 nM crizotinib or 100 nM alectinib, and then cell viability was evaluated by CCK-8 Kit at different time points (0, 24, 48, and 72 h). (E) After 72 h of crizotinib treatment, the phosphorylation levels of NPM1-ALK and its downstream proteins were assessed by WB in APE1 OE and NC ALK+ ALCL cells. (F) WB analysis on ALK oligomerization in APE1 OE, NC, and KD ALK+ALCL cells.

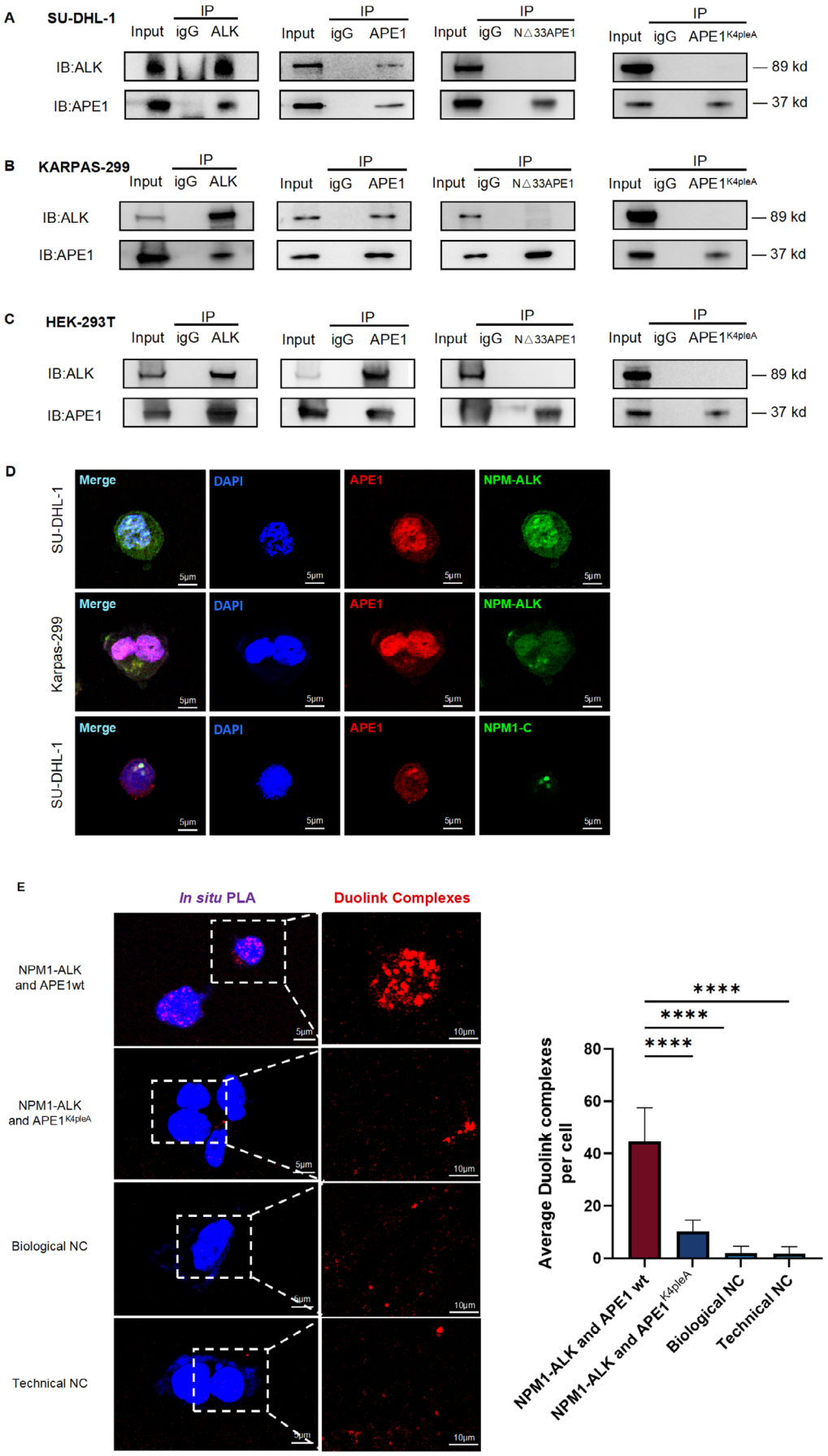

FIGURE 3 | Legend on next page.

FIGURE 3 | APE1 interacts with NPM1-ALK in the nucleus. (A–C) Co-immunoprecipitation (CO-IP) with APE1, NPM1-ALK antibodies, N△33APE1 and APE1^{K4pleA} in SU-DHL-1, Karpas-299 and HEK-293 T cells. (D) Immunofluorescence in ALK+ ALCL cells with APE1, NPM1-ALK and NPM1-C terminal antibody. Scale bar: 5 μm. (E) PLA of NPM-ALK wt and APE1^{K4pleA} shows the interaction happens in the nucleus of HEK 293 T cells. 293 T cells uninfected by NPM1-ALK lentivirus were used as biological negative control (Biological NC) to detect the specificity of primary antibodie; technical negative control (Technical NC) was set with no primary antibody used during the experiment to exclude background signals. Scale bar: 5 μm. Statistical analysis was performed by comparing the data with that of the control group using ordinary one-way ANOVA. *$p < 0.05$, **$p < 0.01$, ***$p < 0.001$, ****$p < 0.0001$.

by WB in NPM1-ALK+ ALCL; the ratio of monomer and oligomer NPM1-ALK is labeled (Figure 4B). The WB assay showed an attenuated phosphorylation of the NPM1-ALK and its downstream signaling pathways in SU-DHL-1 and Karpas-299 cells (Figure 4C). In consideration of the weakened NPM1-ALK oligomers after the mutation at the interaction sites between APE1 and NPM1-ALK, we believe that APE1 Lys27/31/32/35 participates in and assists in the stabilization of NPM1-ALK oligomers, which play an important role in the ALK phosphorylation events. After that, we explored ALK-TKI sensitivity between the APE1^{K4pleA} and APE1 wt groups. Increasing concentrations of each inhibitor were added, and cell viability was assessed by CCK-8. Results show that the IC50 of the APE1^{K4pleA} group was significantly lower than that of the APE1 wt group in two cell lines, especially crizotinib (Figure 4D). We also observed that in SU-DHL-1 cells, the APE1^{K4pleA} group appeared to have a higher apoptotic rate compared to the APE1 wt group under 100 nM crizotinib treatment for 72 h; apoptosis was quantified by a flow detection kit (Figure 4E). WB also showed a diminished phosphorylation of NPM1-ALK in the APE1^{K4pleA} group (Figure 4F).

3.5 | Mutant APE1^{K4pleA} Causes Decreased Tumor Growth and Increased Drug Sensitivity of NPM1-ALK+ ALCL In Vivo

To validate the translational relevance of our findings in vivo, APE1 wt and APE1^{K4pleA} ALK+ALCL subcutaneous graft animal models were constructed. A schematic representation of the in vivo experiment was shown in Figure 5A. Injections of SU-DHL-1 cells at NCG mice resulted in subcutaneous nodules by day 5–7; tumor dimensions were assessed and documented every other day. The growth and drug responsiveness of APE1 wt and APE1^{K4pleA} NPM1-ALK+ ALCL were evaluated in xenograft tumors with crizotinib or placebo. Representative tumors before and after dissection from the placebo and crizotinib groups at the end of experiments are shown in Figure 5B. Body weight and tumor volume changes of mice were shown (Figure 5C,D); we found that xenografts grew slower in the APE1^{K4pleA} groups. After treatment with crizotinib, a more significant tumor regression was achieved in the APE1^{K4pleA} groups, in accord with our in vitro experiments. After dissection of xenografts, IHC staining of pALK and APE1 and WB of NPM1-ALK, pALK, and APE1 showed the same phenomenon (Figure 5E,F).

4 | Discussion

In this paper, we identified a novel factor affecting ALK-driven activity and ALK-TKI sensitivity. Our data suggest that APE1, an interacting protein of the ALK fusion partner NPM1, sustains survival and proliferation signals and reduces ALK-TKI sensitivity of ALK+ ALCL cells through its N-terminal Lys27/31/32/35. In clinical samples, ALK+ ALCL patients with higher APE1 expression levels in tumors were significantly associated with elevated serum LDH levels and more advanced clinical stages at initial diagnosis; their tumors also showed a higher Ki-67 expression and higher ALK-downstream gene activation. To confirm this, we overexpressed APE1 in vitro and found that OE of APE1 promotes the survival and growth of ALK+ ALCL cells, reduces ALK-TKI sensitivity by interacting with NPM1-ALK, and the destruction of the interaction attenuated phosphorylation of NPM1-ALK and enhanced ALK-TKI sensitivity.

With the increasingly understanding of various ALK-fusion associated malignancies, the so-called ALKoma, we are just increasingly aware of the vital role of ALK oligomerization in its activation [33]. In NSCLC, EML4-ALK fusion protein requires ALK dimerization via trimeric coiled-coil domains present in the amino-terminal of EML4 for constitutive ALK activation [34]. Interestingly, we observed a concerted trend of NPM1-ALK oligomer blots with APE1; CO-IP and PLA assay confirmed this interaction. Previous studies have identified the interacting sites of APE1 and NPM1 [32]. Here, we verified for the first time that APE1 interacts with NPM1-ALK fusion protein in the nucleus through its N-terminal Lys27/31/32/35. Afterwards, we found that APE1^{K4pleA}, and not APE1 wt, resulted in a suppressed cell growth and enhanced drug sensitivity, suggesting a role for APE1 signaling in the tumor growth process. These findings explained the heterogeneity of ALCL patients on disease stages at initial diagnosis, progression, and responses to medication.

Therefore, despite most attention being paid to the ALK kinase region [35], we believe the key to controlling ALK phosphorylation events hides in its fusion partners as they play an indispensable role. Here, we verified that the stability of NPM1-ALK oligomerization directly affects ALK activation in ALCL. These findings also have the potential to extend into a broader mechanism of ALK regulation; there must be natural factors in the huge protein interaction network of ALK fusion partners, which can cause steric hindrance through interaction with ALK fusion partners and affect the formation and stability of ALK oligomerization. Targeting fusion partners to affect ALK activation may become a new strategy, not only offering another possible therapeutic approach to ALKoma patients, but also overcoming resistance to ALK-TKIs potentially. As the efficacy of ALK inhibitors may be substantially influenced by mutations, different variants, and gene copy number alterations, focusing on fusion partners could potentially solve these problems [6, 35–37].

Human APE1 N-terminal region is especially conserved in mammals, in charge of nuclear localization and post-translational

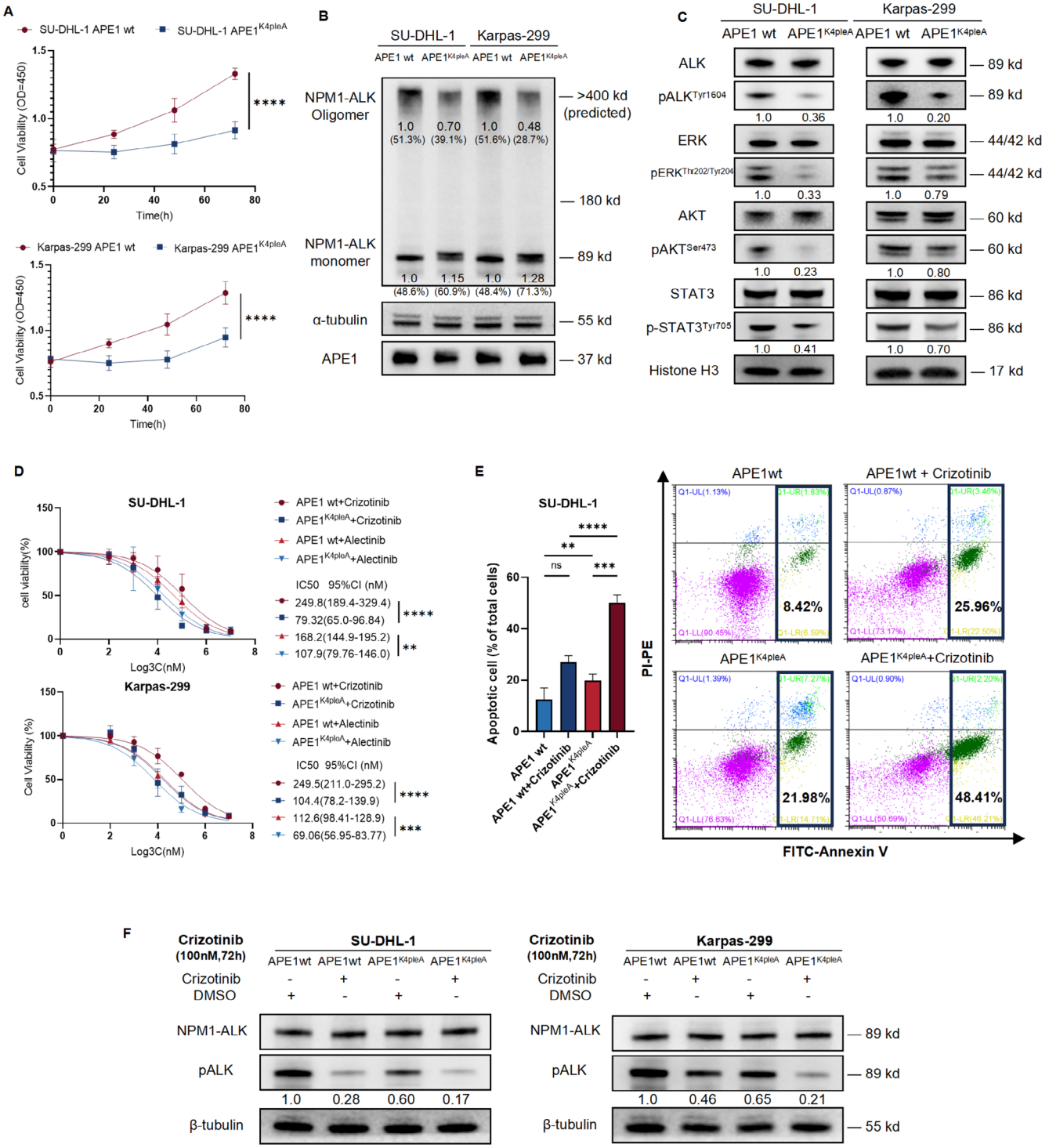

FIGURE 4 | Interaction site mutation of APE1 attenuated phosphorylation of NPM1-ALK and enhanced tumor inhibitory effect of ALK-TKI. (A) Cell viabilities of APE1 wt and APE1^{K4pleA} were evaluated by a CCK-8 kit at the specified time points. (B) WB on APE1 wt and APE1^{K4pleA} cells, NPM1-ALK oligomer, APE1 was assessed. The amount of monomer and oligomer NPM1-ALK is quantified and labeled. (C) WB on APE1 wt and APE1^{K4pleA} ALK+ALCL cell lines, ALK and its downstream biological end-points were assessed. Bands were normalized on Histone H3. (D) ALK-TKI IC50 of APE1 wt and APE1^{K4pleA} ALK+ALCL cells is evaluated using a CCK-8 kit. Cells were treated with crizotinib or alectinib for 72 h. (E) APE1 wt and APE1^{K4pleA} group were treated with 100 nM crizotinib for 72 h in SU-DHL-1 cell; apoptosis was quantified by an apoptosis detection kit, followed by flow cytometry assay. Representative pictures are shown. (F) Phosphorylated NPM1-ALK after crizotinib treatment was assessed by WB. *$p < 0.05$, **$p < 0.01$, ***$p < 0.001$, ****$p < 0.0001$.

modification and protein–protein interactions [38, 39]. Our data suggest a novel fusion protein NPM1-ALK. It is Lys27/31/32/35 of APE1, but not the redox region or endonuclease region, that help sustain NPM1-ALK oligomers and activate the ALK axis. Previous clinical study has certified the antitumor activity of crizotinib in patients with ALK+ ALCL [13]. Hirokazu Nagai

et al. also identified impressive antitumor activity and safety of alectinib clinically [14]. Our study suggests a better curative efficacy for ALK+ ALCL patients with low APE1 expression.

Historically, in NPM1-ALK-positive ALCL, as well as other ALKoma, downstream signaling pathways, such as ERK, AKT, and STAT3 are predominantly driven by ALK signaling [40],

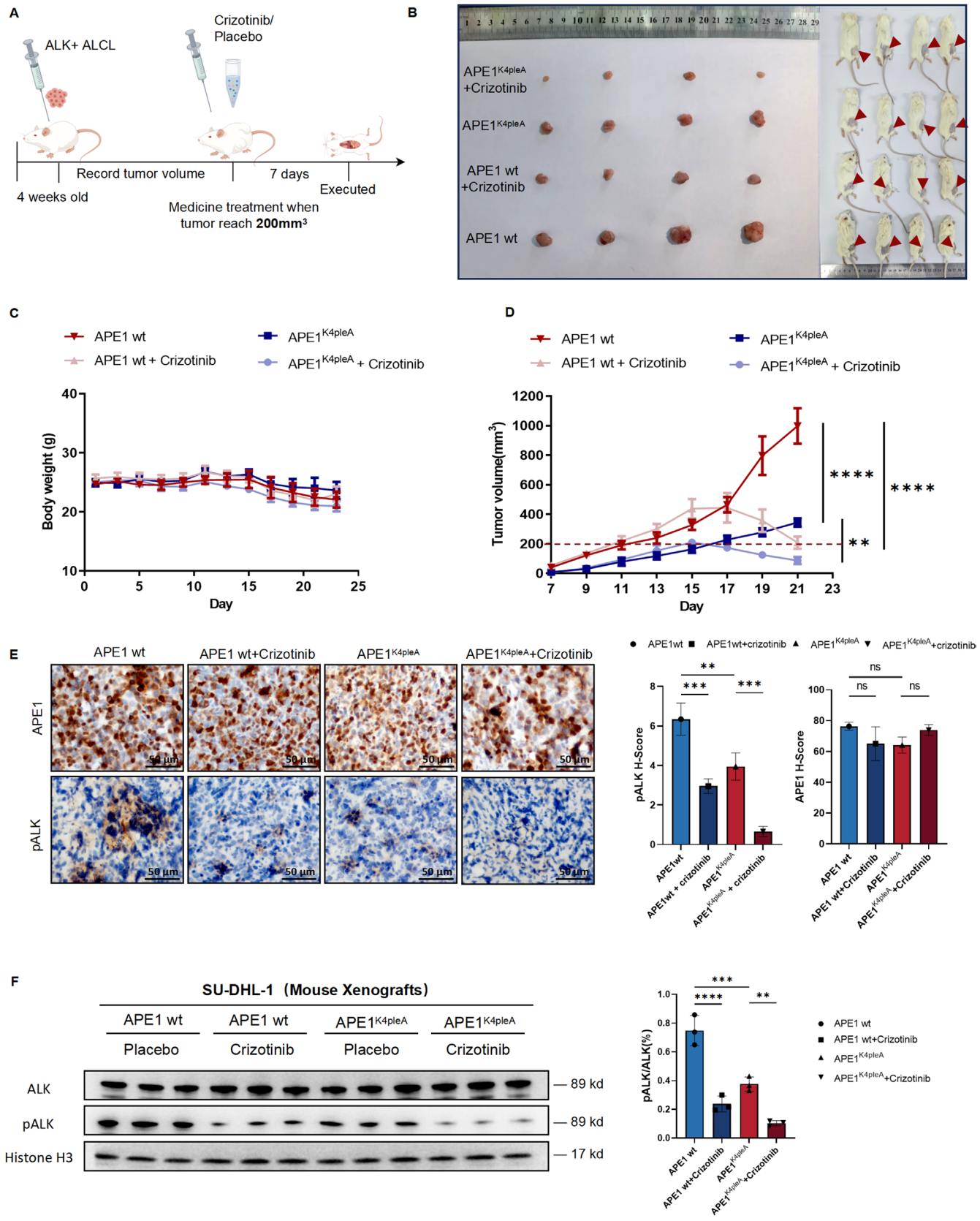

FIGURE 5 | Legend on next page.

FIGURE 5 | Mutant APE1^{K4pleA} causes decreased tumor growth and increased drug sensitivity of NPM1-ALK+ ALCL in vivo. (A) Schematic representation of the in vivo experiment. Male NCG mice were implanted with SU-DHL-1 cells after 3 days of acclimatization. When tumor volume reached 200 mm^3, mice were treated with crizotinib (50 mg/kg) or a placebo by intragastric administration every day for a week. Mice were euthanized and tumors were surgically dissected at a humane endpoint. 6 mice per group, maximum and minimum tumors within the group were excluded. (B) Representative pictures of tumors from each group before and after dissection. (C, D) Body weight and tumor volume of mice, which were measured every other day. (E) Representative images of immunohistochemical staining of APE1 and pALK of the xenografts. Scale bars, 50 μm. The statistical analysis was presented following images. (F) WB analysis performed on xenografts different group, NPM1-ALK, pALK, and APE1 were assessed. *$p < 0.05$, **$p < 0.01$, ***$p < 0.001$, ****$p < 0.0001$.

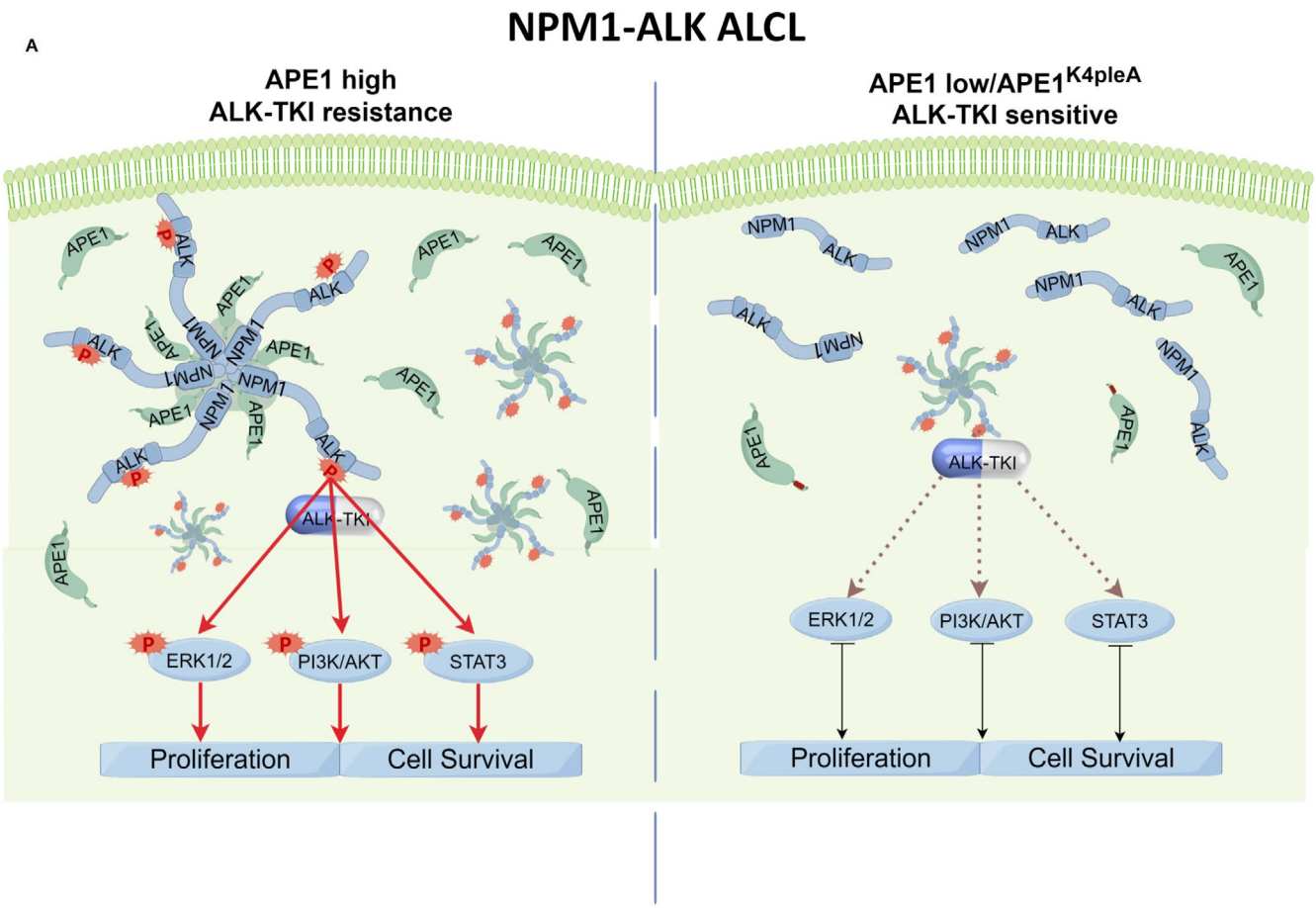

FIGURE 6 | Schematic diagram of APE1 affecting the NPM1-ALK fusion protein in ALK+ ALCL. (A) NPM1's interaction protein APE1 improves cell proliferation and reduce ALK-TKI sensitivity in NPM1-ALK ALCL by stabilizing its oligomerization, and APE1^{K4pleA} could enhance cytotoxic effects of ALK-TKI in ALK+ ALCL.

APE1 help strengthen this signal through interaction with NPM1-ALK. While secondary regulators (e.g., RAS/BCAP for AKT; JAK/Src for STAT3) may contribute to baseline pathway activation and were intermittently activated, their influence is minimal in this context and cannot be entirely excluded. The primary mechanism of action of ALK-TKI involves direct suppression of ALK kinase activity, thereby attenuating downstream pAKT/pSTAT3 signaling; this aligns with the established role of NPM1-ALK as the central oncogenic driver in this subtype of ALCL. That explains why high concentrations of ALK-TKIs might inhibit the activation of ALK downstream pathways even in the condition of overexpressed APE1. Meanwhile, a certain phenomenon has been observed by IC-50 assay that OE of APE1 could reduce ALK-TKI sensitivity. It is well known that in NPM1-ALK-positive ALCL, higher ALK activity signifies stronger tumor-driven activity, leading to enhanced cellular proliferation. Interestingly, this study also found that in clinical samples, tumors with higher APE1 expression exhibited elevated Ki-67 expression levels, and patients were more likely to present with advanced-stage disease at initial diagnosis. These findings further validate the critical role of APE1 in NPM1-ALK-driven tumors.

Many ongoing clinical researches have focused on the heterogeneity of ALK+ NSCLC patients [41, 42]. However, currently, there remains a lack of large-scale prospective clinical data on the heterogeneity of ALK+ ALCL patients. The study herein offers a step in this direction and employs more precise identification and therapeutic strategies for ALCL patients. Notably, the clinical application of these approaches still faces some

challenges in China, where ALK-TKIs are not yet approved for first-line treatment of NPM1-ALK+ ALCL. Consequently, clinical data on their application in this specific subtype remain unavailable. Our future research will focus on elucidating the influences of APE1 on ALK-TKIs and the therapeutic responses clinically.

In summary, this paper demonstrated that NPM1's interaction protein APE1 improves cell growth and reduce ALK-TKI sensitivity in NPM1-ALK ALCL by stabilizing its oligomerization, and $APE1^{K4pleA}$ could enhance cytotoxic effects of ALK-TKI in ALK+ ALCL (Figure 6A). By focusing on the steric hindrance effect of natural proteins that can form stable structures with ALK fusion partners on the formation of ALK fusion proteins, we can control ALK phosphorylation events more effectively and identify patients more accurately.

Author Contributions

Mengxia Li: conceptualization, resources, supervision. **Zheng Liu:** data curation, formal analysis, investigation, methodology, project administration, software, visualization, writing – original draft. **Xinming Jing:** data curation, funding acquisition, methodology, resources, writing – original draft. **Dong Li:** investigation, resources, supervision, validation, visualization, writing – review and editing. **Lingbo Bao:** data curation, project administration. **Yi Liu:** investigation, methodology. **Ruyi Hang:** software, visualization. **Xunjie Kuang:** methodology, supervision. **Ziqi Jiang:** software, visualization. **Xiaoyan Dai:** data curation, investigation. **Xueling Tong:** methodology. **Gianluca Tell:** supervision, writing – review and editing.

Acknowledgments

We thank all of the financial supporters for this research. We gratefully acknowledge Yi Cheng for kindly providing cell lines. We extend our sincere thanks to Yuxin Yang for their expert assistance in coordinating pathological sample collection and processing. Special appreciation is given to Xin Guo for her contributions to plasmid design, viral vector construction, and validation experiments. These collective efforts significantly advanced the experimental progress of this study.

Ethics Statement

Approval of the research protocol by an Institutional Reviewer Board: All protocols and informed consent in this study were approved by the Ethics Committee of Army Medical Center of PLA, with ratification No: 2024 (408). Animal Studies: All procedures involving mice in this study are approved by the Laboratory Animal Welfare and Ethics Committee of the Army Medical University (AMUWEC20237160).

Consent

Protocol, informed consent form was approved by the Ethics committee of Army Medical Center of PLA.

Conflicts of Interest

The authors declare no conflicts of interest.

References

1. X. Zhang, P. Chien, S. Nam, and C. Heo, "Anaplastic Large Cell Lymphoma: Molecular Pathogenesis and Treatment," *Cancers* 14 (2022): 1650.

2. M. Shiota, J. Fujimoto, T. Semba, H. Satoh, T. Yamamoto, and S. Mori, "Hyperphosphorylation of a Novel 80 kDa Protein-Tyrosine Kinase Similar to Ltk in a Human Ki-1 Lymphoma Cell Line, AMS3," *Oncogene* 9 (1994): 1567–1574.

3. E. Bergaggio, W. Tai, A. Aroldi, et al., "ALK Inhibitors Increase ALK Expression and Sensitize Neuroblastoma Cells to ALK.CAR-T Cells," *Cancer Cell* 41 (2023): 2100–2116.

4. M. Kalinova, M. Mrhalova, E. Kabickova, et al., "Molecular Screening in Anaplastic Lymphoma Kinase–Positive Anaplastic Large Cell Lymphoma: Anaplastic Lymphoma Kinase Analysis, Next-Generation Sequencing Fusion Gene Detection, and T-Cell Receptor Immunoprofiling," *Modern Pathology* 37 (2024): 100428.

5. J. Luedersen, U. Z. Stadt, J. Richter, et al., "VariantALK-Fusion Positive Anaplastic Large Cell Lymphoma (ALCL): A Population-Based Paediatric Study of theNHL-BFM Study Group," *British Journal of Haematology* 204 (2024): 1894–1898.

6. M. Elshatlawy, J. Sampson, K. Clarke, and R. Bayliss, "EML4-ALK Biology and Drug Resistance in Non-Small Cell Lung Cancer: A New Phase of Discoveries," *Molecular Oncology* 17 (2023): 950–963.

7. J. E. Herrera, J. J. Correia, A. E. Jones, and M. O. J. Olson, "Sedimentation Analyses of the Salt- and Divalent Metal Ion-Induced Oligomerization of Nucleolar Protein B23," *Biochemistry* 35 (1996): 2668–2673.

8. M. Saluri, A. Leppert, G. V. Gese, et al., "A 'Grappling Hook' Interaction Connects Self-Assembly and Chaperone Activity of Nucleophosmin 1," *PNAS Nexus* 2 (2023): pgac303.

9. S. S. Rajan, A. D. Amin, L. Li, et al., "The Mechanism of Cancer Drug Addiction in ALK-Positive T-Cell Lymphoma," *Oncogene* 39 (2020): 2103–2117.

10. V. R. Belum, K. Marulanda, C. Ensslin, et al., "Alopecia in Patients Treated With Molecularly Targeted Anticancer Therapies," *Annals of Oncology* 26 (2015): 2496–2502.

11. C. Laurent, A. Nicolae, C. Laurent, et al., "Gene Alterations in Epigenetic Modifiers and JAK-STAT Signaling Are Frequent in Breast Implant-Associated ALCL," *Blood* 135 (2019): 360–370.

12. M. Menotti, C. Ambrogio, T. Cheong, et al., "Wiskott–Aldrich Syndrome Protein (WASP) is a Tumor Suppressor in T Cell Lymphoma," *Nature Medicine* 25 (2019): 130–140.

13. Y. P. Mossé, M. S. Lim, S. D. Voss, et al., "Safety and Activity of Crizotinib for Paediatric Patients With Refractory Solid Tumours or Anaplastic Large-Cell Lymphoma: A Children's Oncology Group Phase 1 Consortium Study," *Lancet Oncology* 14 (2013): 472–480.

14. R. Fukano, T. Mori, M. Sekimizu, et al., "Alectinib for Relapsed or Refractory Anaplastic Lymphoma Kinase-Positive Anaplastic Large Cell Lymphoma: An Open-Label Phase II Trial," *Cancer Science* 111 (2020): 4540–4547.

15. G. Rindone, A. Aroldi, E. Bossi, et al., "A Monocentric Analysis of the Long-Term Safety and Efficacy of Crizotinib in Relapsed/Refractory ALK+ Lymphomas," *Blood Advances* 7 (2023): 314–316.

16. R. Russell-Jones, "World Health Organization Classification of Hematopoietic and Lymphoid Tissues: Implications for Dermatology," *Journal of the American Academy of Dermatology* 48 (2003): 93–102.

17. R. Wu and M. S. Lim, "Updates in Pathobiological Aspects of Anaplastic Large Cell Lymphoma," *Frontiers in Oncology* 13 (2023): 1241532.

18. J. Wang, L. Zhong, W. Lin, et al., "JAK/STAT3 Signaling Activation Related to Distinct Clinicopathologic Features in Systemic ALK– Anaplastic Large Cell Lymphomas," *American Journal of Surgical Pathology* 47 (2023): 55–64.

19. M. Poletto, M. C. Malfatti, D. Dorjsuren, et al., "Inhibitors of the Apurinic/Apyrimidinic Endonuclease 1 (APE1)/nucleophosmin (NPM1) Interaction That Display Anti-Tumor Properties," *Molecular Carcinogenesis* 55 (2016): 688–704.

20. C. Vascotto, D. Fantini, M. Romanello, et al., "APE1/Ref-1 Interacts With NPM1 Within Nucleoli and Plays a Role in the rRNA Quality Control Process," *Molecular and Cellular Biology* 29 (2009): 1834–1854.

21. G. Tell, D. Fantini, and F. Quadrifoglio, "Understanding Different Functions of Mammalian AP Endonuclease (APE1) as a Promising Tool for Cancer Treatment," *Cellular and Molecular Life Sciences* 67 (2010): 3589–3608.

22. K. A. Robertson, H. A. Bullock, Y. Xu, et al., "Altered Expression of Ape1/Ref-1 in Germ Cell Tumors and Overexpression in NT2 Cells Confers Resistance to Bleomycin and Radiation," *Cancer Research* 61 (2001): 2220–2225.

23. Y. Du, Y. Zhou, X. Yan, et al., "APE1 Inhibition Enhances Ferroptotic Cell Death and Contributes to Hepatocellular Carcinoma Therapy," *Cell Death and Differentiation* 31 (2024): 431–446.

24. M. C. Malfatti, A. Bellina, G. Antoniali, and G. Tell, "Revisiting Two Decades of Research Focused on Targeting APE1 for Cancer Therapy: The Pros and Cons," *Cells* 12 (2023): 1895.

25. G. Antoniali, E. Dalla, G. Mangiapane, et al., "APE1 Controls DICER1 Expression in NSCLC Through miR-33a and miR-130b," *Cellular and Molecular Life Sciences* 79 (2022): 446.

26. A. V. Popov, A. V. Endutkin, D. D. Yatsenko, et al., "Molecular Dynamics Approach to Identification of New OGG1 Cancer-Associated Somatic Variants With Impaired Activity," *Journal of Biological Chemistry* 296 (2021): 100229.

27. M. L. Hegde, T. K. Hazra, and S. Mitra, "Functions of Disordered Regions in Mammalian Early Base Excision Repair Proteins," *Cellular and Molecular Life Sciences* 67 (2010): 3573–3587.

28. D. Fantini, C. Vascotto, D. Marasco, et al., "Critical Lysine Residues Within the Overlooked N-Terminal Domain of Human APE1 Regulate Its Biological Functions," *Nucleic Acids Research* 38 (2010): 8239–8256.

29. N. Moor, E. I. Vasil, and O. Lavrik, "Functional Role of N-Terminal Extension of Human AP Endonuclease 1 in Coordination of Base Excision DNA Repair via Protein–Protein Interactions," *International Journal of Molecular Sciences* 21 (2020): 3122.

30. M. Li, X. Yang, X. Lu, et al., "APE1 Deficiency Promotes Cellular Senescence and Premature Aging Features," *Nucleic Acids Research* 46 (2018): 5664–5677.

31. N. Hirai, T. Sasaki, S. Okumura, Y. Minami, S. Chiba, and Y. Ohsaki, "Monomerization of ALK Fusion Proteins as a Therapeutic Strategy in ALK-Rearranged Non-Small Cell Lung Cancers," *Frontiers in Oncology* 10 (2020): 419.

32. G. Mangiapane, M. Notarangelo, G. Canarutto, et al., "The DNA-Repair Protein APE1 Participates With hnRNPA2B1 to Motif-Enriched and Prognostic miRNA Secretion," *Oncogene* 43 (2024): 1861–1876.

33. M. W. Richards, E. W. Law, L. P. Rennalls, et al., "Crystal Structure of EML1 Reveals the Basis for Hsp90 Dependence of Oncogenic EML4-ALK by Disruption of an Atypical β-Propeller Domain," *Proceedings of the National Academy of Sciences of the United States of America* 111 (2014): 5195–5200.

34. M. W. Richards, L. O'Regan, D. Roth, et al., "Microtubule Association of EML Proteins and the EML4-ALK Variant 3 Oncoprotein Require an N-Terminal Trimerization Domain," *Biochemical Journal* 467 (2015): 529–536.

35. J. L. Schneider, J. J. Lin, and A. T. Shaw, "ALK-Positive Lung Cancer: A Moving Target," *Nature Cancer* 4 (2023): 330–343.

36. A. J. Cooper, L. V. Sequist, and J. J. Lin, "Third-Generation EGFR and ALK Inhibitors: Mechanisms of Resistance and Management," *Nature Reviews. Clinical Oncology* 19 (2022): 499–514.

37. A. Shiba-Ishii, T. W. Johnson, I. Dagogo-Jack, et al., "Analysis of Lorlatinib Analogs Reveals a Roadmap for Targeting Diverse Compound Resistance Mutations in ALK-Positive Lung Cancer," *Nature Cancer* 3 (2022): 710–722.

38. E. B. Jackson, "Analysis of Nuclear Transport Signals in the Human Apurinic/Apyrimidinic Endonuclease (APE1/Ref1)," *Nucleic Acids Research* 33 (2005): 3303–3312.

39. G. Antoniali, F. Serra, L. Lirussi, et al., "Mammalian APE1 Controls miRNA Processing and Its Interactome Is Linked to Cancer RNA Metabolism," *Nature Communications* 8 (2017): 797.

40. S. Zhao, J. Li, Q. Xia, K. Liu, and Z. Dong, "New Perspectives for Targeting Therapy in ALK-Positive Human Cancers," *Oncogene* 42 (2023): 1959–1969.

41. J. M. Heuckmann, M. Hölzel, M. L. Sos, et al., "ALK Mutations Conferring Differential Resistance to Structurally Diverse ALK Inhibitors," *Clinical Cancer Research* 17 (2011): 7394–7401.

42. M. Guan, J. Xu, and Q. Shi, "Molecular Determinants of Clinical Outcomes for Anaplastic Lymphoma Kinase-Positive Non-Small Cell Lung Cancer in Chinese Patients: A Retrospective Study," *Cancer Genetics* 270-271 (2023): 32–38.

Supporting Information

Additional supporting information can be found online in the Supporting Information section.